International Journal of Engineering Inventions
e-ISSN: 2278-7461, p-ISSN: 2319-6491
Volume 14, Issue 11 [November 2025] PP: 136-146

Performance Evaluation of Protective Coatings on Carbon Steel Exposed to Salalah's Climatic Conditions

Kumaradhas Paulian[a1], Venkatesan Tharanipathy[a], Naveen Prasad[a], Vijayanand Manickam[a] .
Corresponding author: Kumaradhas Paulian

Abstract
Corrosion poses a significant challenge for carbon steel structures, particularly in coastal regions with high salinity and humidity. This study investigates the corrosion behavior of carbon steel under the unique environmental conditions of Salalah, Oman—a region characterized by high humidity, frequent rainfall, and salty air, especially during the Khareef (monsoon) season. The research was conducted in two phases: first, by exposing uncoated carbon steel samples to Salalah's open-air environment to monitor natural corrosion progression; and second, by evaluating the effectiveness of protective coatings—Zinc, Acrylic, and Normal Paint—applied to similar samples.
Corrosion rates were assessed through weight loss measurements, optical microscopy, and mechanical tests including hardness, impact strength, and wear resistance. The results indicate that the combination of chloride ions, prolonged moisture exposure, and fluctuating temperatures significantly accelerates corrosion. Among the tested coatings, zinc offered the most effective and durable protection, maintaining both structural integrity and corrosion resistance throughout the ten-week test period. Acrylic coatings showed moderate short-term performance but deteriorated over time, while normal paint offered minimal protection.
The findings highlight the importance of appropriate materials selection and protective strategies—such as coatings and cathodic protection—for enhancing the longevity of carbon steel structures in aggressive coastal environments like Salalah. These insights offer valuable guidance for engineers, infrastructure planners, and industries aiming to implement cost-effective and sustainable corrosion mitigation solutions.
Keywords: *Corrosion, Coatings, Salalah*

Date of Submission: 13-11-2025 Date of acceptance: 27-11-2025

I. Introduction

Corrosion of carbon steel in coastal environments poses a significant challenge to infrastructure, particularly in regions characterized by high humidity, salinity, and temperature fluctuations. Salalah, Oman, situated along the southern coast of the Arabian Peninsula, experiences unique climatic conditions during the Khareef (monsoon) season, including increased humidity, frequent rainfall, and salty air. These factors contribute to accelerated corrosion rates of exposed metal structures, necessitating effective mitigation strategies.

Recent studies have highlighted the detrimental effects of marine atmospheric conditions on carbon steel. For instance, Alcántara et al. (2017) reviewed the corrosion behavior of carbon steel in marine atmospheres, emphasizing the role of chloride ions and moisture in initiating and propagating corrosion processes. Similarly, López-Ortega et al. (2019) evaluated protective coatings for high-corrosivity atmospheres, underscoring the importance of selecting appropriate materials to enhance the longevity of steel structures in offshore applications. Popescu et al. (2022) investigated the influence of seawater corrosion on the structure and magnetic properties of carbon steels, noting the protective role of zinc in mitigating corrosion effects. Gao et al. (2023) examined the corrosion resistance of low-alloy steel in marine environments, indicating that acrylic-based coatings may degrade under prolonged exposure to aggressive conditions. Montemor (2014) discussed functional and smart coatings for corrosion protection, highlighting the inadequacy of standard paints in harsh marine environments.

In the context of protective measures, various coatings have been assessed for their efficacy in preventing corrosion. Zinc coatings, known for their sacrificial protection properties, have been extensively studied. A study by Popescu et al. (2022) investigated the influence of seawater corrosion on the structure and magnetic properties of carbon steels, noting the protective role of zinc in mitigating corrosion effects. Acrylic coatings, while offering moderate protection, have shown limitations over time. Research by Gao et al. (2023) examined the corrosion resistance of low-alloy steel in marine environments, indicating that acrylic-based coatings may degrade under prolonged exposure to aggressive conditions. Normal paints, often used as cost-effective solutions, provide minimal protection against corrosion. A comprehensive review by Montemor (2014) discussed functional and

smart coatings for corrosion protection, highlighting the inadequacy of standard paints in harsh marine environments.

The current study aims to investigate the corrosion behavior of carbon steel under the environmental conditions of Salalah, Oman, and evaluate the effectiveness of various protective coatings, including zinc, acrylic, and normal paint. By exposing uncoated and coated carbon steel samples to Salalah's open-air environment, this research seeks to provide insights into the progression of corrosion and the performance of different protective strategies. The findings are expected to contribute valuable information for engineers and infrastructure planners in developing cost-effective and sustainable corrosion mitigation solutions for coastal regions.

II. Materials and Methods

The experimental investigation on the corrosion behavior of carbon steel was conducted over a duration of ten weeks. Throughout this period, consistent monitoring and systematic experimentation were carried out on all test specimens to ensure data reliability.

Low-carbon steel was selected as the base material due to its widespread use in structural applications where high hardness or intrinsic corrosion resistance is not critical. The chemical composition of the carbon steel used in this study was as follows: Carbon (C) content ranging from 0.05% to 0.25%, Manganese (Mn) between 0.4% and 0.7%, Silicon (Si) from 0.1% to 0.3% (in specific grades), Sulfur (S) less than 0.05%, and Phosphorus (P) 0.04% or lower. The remainder of the composition, accounting for more than 98% of the total mass, consisted predominantly of Iron (Fe).

The specimens, each measuring 50 mm × 25 mm × 5 mm, were subjected to three different environmental conditions: (1) no spray (control), (2) exposure to a 4% sodium chloride (NaCl) spray, and (3) exposure to a 36% hydrochloric acid (HCl) spray. Additionally, three types of protective coatings—paint, zinc, and acrylic—were applied to evaluate their effectiveness against corrosion under these conditions. These conditions were intended to represent the environmental stressors commonly encountered in coastal regions such as Salalah, Oman.

Corrosion Mechanism

Corrosion of carbon steel in coastal environments such as Salalah is primarily driven by electrochemical reactions accelerated by the presence of moisture, salt (chloride ions), and oxygen. When steel is exposed to humid air, especially air rich in sodium chloride from sea spray, a thin film of moisture forms on the metal surface. This film acts as an electrolyte, enabling the flow of ions between anodic (metal-losing) and cathodic (electron-accepting) sites on the steel surface. At the anodic sites, iron oxidizes to Fe^{2+} (iron ions), while at the cathodic sites, oxygen is reduced—typically forming hydroxide ions (OH^-). This process initiates rust formation.

In saline environments like Salalah, chloride ions (Cl^-) play a particularly aggressive role. These ions break down the passive iron oxide layer that might otherwise slow corrosion. Chlorides also stabilize the formation of akaganeite (β-FeOOH)**,** a rust phase that forms under acidic, chloride-rich conditions and is known for trapping chloride ions within its structure. This makes corrosion self-sustaining: akaganeite retains and recycles chloride ions, keeping the steel surface chemically active and continuously corroding. Moreover, high humidity ensures persistent wetting, while temperature fluctuations accelerate the electrochemical reactions. As a result, steel exposed to these conditions exhibits pitting, under-film corrosion, and general material loss over time.

- Basic Electrochemical Corrosion of Iron (Steel)

Anodic Reaction (Iron oxidation):
At anodic sites, iron is oxidized:

$$\mathrm{Fe} \rightarrow \mathrm{Fe}^{2+} + 2e^-$$

Cathodic Reaction (Oxygen reduction in neutral/alkaline solution):

$$\mathrm{O_2} + 2\mathrm{H_2O} + 4e^- \rightarrow 4\mathrm{OH}^-$$

Overall Reaction (in the presence of water and oxygen):

$$2\mathrm{Fe} + \mathrm{O_2} + 2\mathrm{H_2O} \rightarrow 2\mathrm{Fe(OH)_2}$$

- Formation of Rust (Iron Oxides/Hydroxides)

The initial ferrous hydroxide Fe(OH)2 can further oxidize to ferric hydroxide:

$$4\mathrm{Fe(OH)_2} + \mathrm{O_2} + 2\mathrm{H_2O} \rightarrow 4\mathrm{Fe(OH)_3}$$

Ferric hydroxide dehydrates to form iron oxides, which are collectively known as rust:

$$\mathrm{Fe(OH)_3} \rightarrow \mathrm{Fe_2O_3} \cdot n\mathrm{H_2O}$$

- Chloride-Induced Corrosion – Akaganeite Formation

In coastal regions, chloride ions penetrate the corrosion product layers and destabilize protective oxides. Under these conditions, a chloride-containing rust phase known as akaganeite (β\betaβ-FeOOH) can form:

$$Fe^{2+} + Cl^- + O_2 + H_2O \rightarrow \beta\text{-}FeOOH + H^+$$

- Akaganeite traps chloride ions in its structure, leading to sustained corrosion.
- The production of H+ ions also lowers pH, accelerating further metal dissolution.

These reactions demonstrate why high humidity and chloride content, as found in coastal atmospheres, make carbon steel especially vulnerable to corrosion. Understanding these mechanisms is key to choosing proper protective coatings or cathodic protection systems in such environments.

III. Results and Discussion

Hardness Test

The Brinell Hardness Number (BHN) values of carbon steel samples were recorded weekly over a ten-week period under three different environmental conditions and three different protective coatings. The metal sample was positioned on the testing machine, and a 2.5 mm diameter steel ball was pressed into its surface under a load of 187.5 kgf. The load was applied for a standardized duration of 10 to 15 seconds to ensure the formation of a stable and consistent indentation.The variations in BHN across the test duration are presented in Table 1.

Table 1: Brinell Hardness Number (BHN) for carbon steel samples under different exposure conditions

Week	No Spray (Control)	NaCl Spray (4%)	HCl Spray (36%)	Paint	Zinc	Acrylic
1	144	143	142	144	144	144
2	144	141	141	144	144	143
3	141	141	140	143	144	143
4	140	140	139	143	143	142
5	139	140	139	142	143	142
6	139	139	139	141	143	142
7	137	139	138	141	142	141
8	137	137	136	140	142	141
9	136	137	134	140	141	140
10	135	136	134	139	141	140

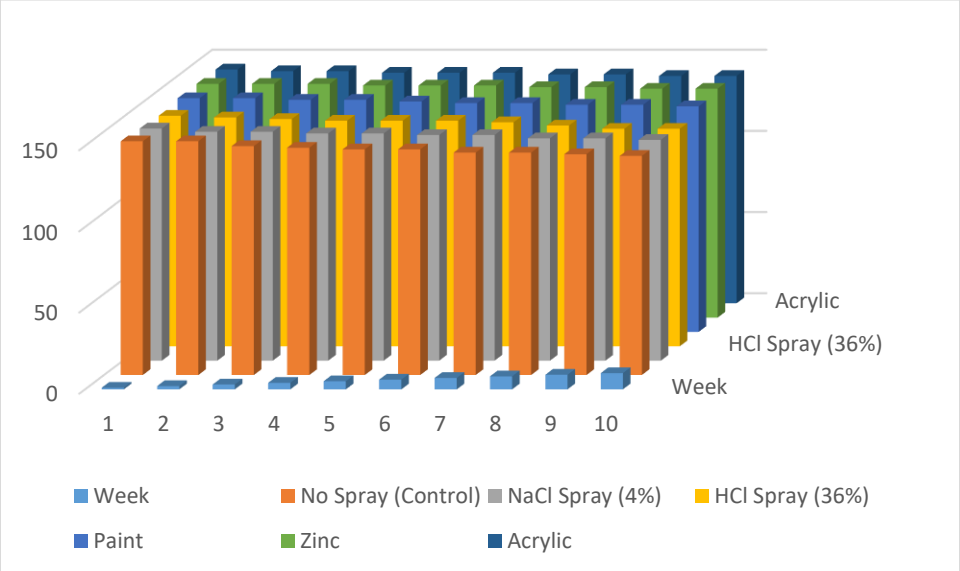

The table 2 presents data from a 10-week corrosion resistance study conducted on materials exposed to various environmental conditions. Each column represents a different treatment or coating method, while the rows show the material integrity readings over time, likely measured in consistent units such as microns. The "No Spray (Control)" group, which was not exposed to any chemicals, serves as a baseline and shows a gradual decline from 144 in Week 1 to 135 in Week 10, indicating natural degradation. The "NaCl Spray (4%)" group, simulating exposure to a saltwater environment, displays a slightly faster rate of degradation, ending at 136 by Week 10. The "HCl Spray (36%)" group, representing an aggressive acidic environment, shows the most significant decline, dropping to 134, which confirms the strong corrosive effect of hydrochloric acid.

In contrast, the protective coatings demonstrate varying levels of effectiveness. The paint-coated samples show moderate protection, with values decreasing from 144 to 139. Zinc-coated samples perform notably well, maintaining values between 144 and 141, indicating strong resistance to corrosion, likely due to the galvanic protection offered by zinc. Overall, the data suggests that zinc coatings provide the best protection against corrosion, while hydrochloric acid exposure results in the most severe material degradation.

Corrosion Rate (CR)

The corrosion rate (CR) quantifies the material loss due to corrosion over a given period and is expressed in millimeters per year (mm/y). The formula used for calculating the corrosion rate is:

$$\mathrm{CR} = \frac{k \cdot m_{\mathrm{loss}}}{A \cdot t \cdot \rho}$$

Where:

- **CR** = Corrosion Rate (mm/y)
- **k** = A constant (8.76×10^4) to convert the units appropriately so that the corrosion rate is expressed in mm/year when other variables are in the specified units.
- $\mathbf{m_{loss}}$ = Mass loss of the metal in grams (g), calculated as the difference between the initial mass (m_o) and the final mass (m_t) after exposure to the corrosive environment.
- **A** = Surface area of the exposed material in square centimeters (cm^2).
- **t** = Time of exposure in hours (h).
- **ρ** = Density of the material in grams per cubic centimeter (g/cm^3).

Table 2: Corrosion Rate of Samples

Wk	δw NaCl Spray	C.R mm/year	δw HCL spray	C.R mm/year	δw Without spray	C.R mm/year
1	0.06	0.19927	0.07	0.23248	0.02	0.06642
2	0.14	0.23248	0.23	0.38194	0.05	0.08303
3	0.23	0.25463	0.37	0.40961	0.21	0.23248
4	0.42	0.34873	0.48	0.39854	0.37	0.30721
5	0.56	0.37197	0.72	0.47825	0.42	0.27898
6	0.62	0.34319	0.94	0.52032	0.48	0.26570
7	0.68	0.32263	1.08	0.51241	0.53	0.25146
8	0.74	0.30721	1.19	0.49403	0.61	0.25324
9	0.87	0.32105	1.33	0.49080	0.73	0.26939
10	0.96	0.31884	1.46	0.48490	0.78	0.25905
	δw	C.R	δw	C.R	δw	C.R
	Epoxy Paint	mm/year	Zinc Coating	mm/year	Acrylic Coating	mm/year
1	0.015	0.04982	0.01	0.03321	0.012	0.03985
2	0.018	0.02989	0.014	0.02325	0.016	0.02657
3	0.024	0.02657	0.018	0.01993	0.022	0.02436
4	0.031	0.02574	0.021	0.01744	0.026	0.02159
5	0.038	0.02524	0.025	0.01661	0.031	0.02059
6	0.045	0.02491	0.028	0.01550	0.035	0.01937
7	0.052	0.02467	0.031	0.01471	0.042	0.01993
8	0.062	0.02574	0.034	0.01412	0.053	0.02200
9	0.071	0.02620	0.037	0.01365	0.064	0.02362
10	0.083	0.02757	0.042	0.01395	0.068	0.02258

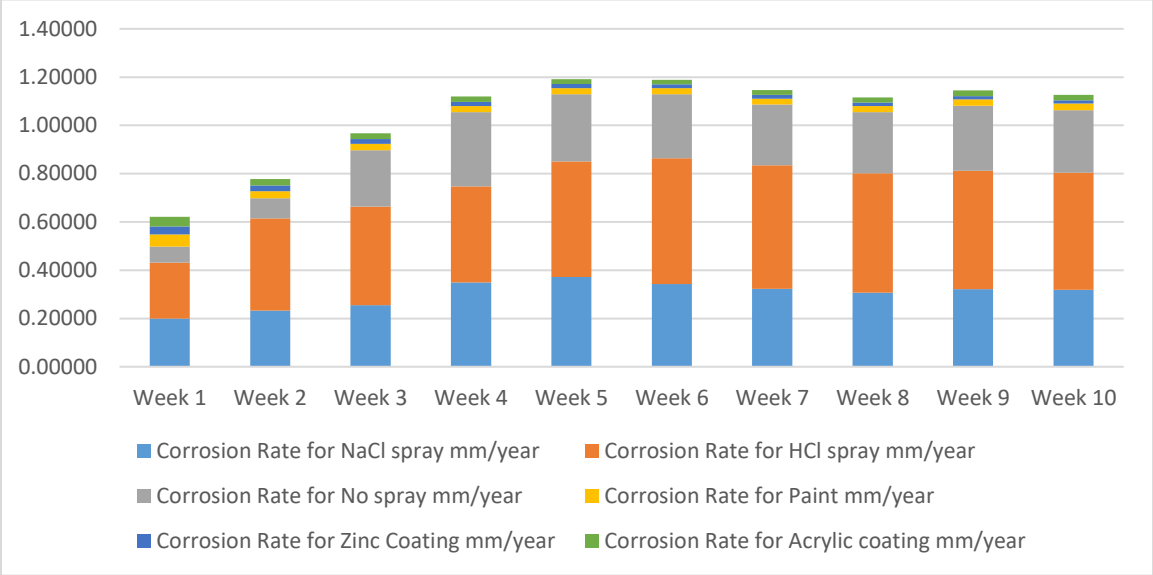

The corrosion rate results over a 10-week exposure period reveal significant differences in the protective effectiveness of various surface treatments and environmental conditions. Among the uncoated specimens, the sample exposed to 36% hydrochloric acid (HCl) spray exhibited the highest corrosion rates across all weeks, reaching a peak of 0.52032 mm/year in Week 6. This highlights the aggressive nature of acidic environments in accelerating metal degradation. The NaCl spray (4%) condition showed moderate corrosion behavior, with rates ranging from 0.19927 mm/year **to** 0.37197 mm/year, indicating that chloride-induced corrosion, while less severe than acid exposure, still contributes to significant material loss over time. The control group (without spray) displayed the lowest corrosion rates among the uncoated samples, peaking at 0.30721 mm/year in Week 4, confirming the detrimental effect of corrosive agents when compared to ambient conditions.

In contrast, the specimens treated with surface coatings demonstrated markedly lower corrosion rates, underscoring the importance of protective barriers in corrosion mitigation. Zinc coating consistently exhibited the lowest corrosion rates, ranging from 0.01365 to 0.03321 mm/year**,** which is attributed to its sacrificial protection mechanism that inhibits corrosion of the underlying substrate. Acrylic coatings also performed well, although with slightly higher corrosion rates than zinc, ranging between 0.01937 and 0.03985 mm/year**.** Interestingly, while epoxy paint offered good initial protection, its corrosion rate increased gradually over time, from 0.04982 mm/year in Week 1 to 0.02757 mm/year in Week 10, suggesting potential degradation or porosity in the coating over prolonged exposure.

Overall, the data clearly indicate that surface coatings significantly reduce the corrosion rate**,** with zinc offering the most consistent protection. Meanwhile, uncoated metals exposed to aggressive environments like HCl suffer substantial mass loss, affirming the need for protective strategies in corrosive settings.

Optical Microscopic Study

An optical microscope equipped with a 10× magnification lens was utilized to examine the microstructural features of the samples. The analysis was conducted using the UEye Cockpit imaging software, which facilitated real-time observation and image capture for documentation and further analysis.

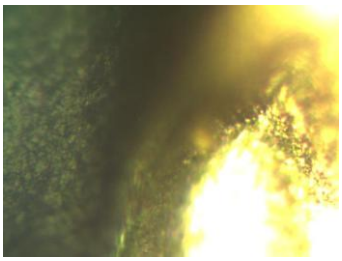

Fig 1: Optical Image of Unexposed Carbon Steel

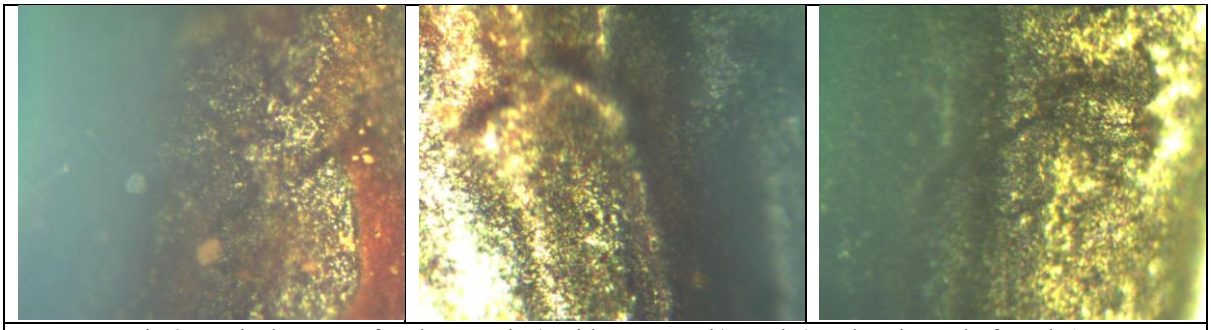

Fig 2: Optical Image of carbon steel: a) without spray b)NaCl c)HCl at the end of week 1

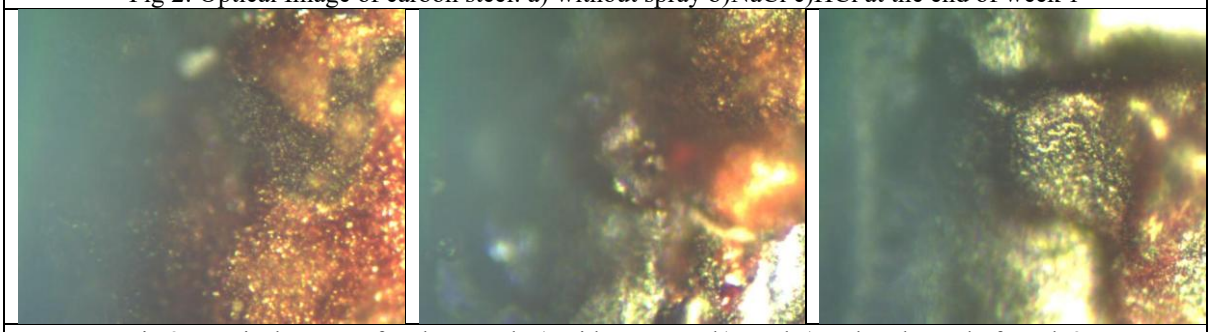

Fig 3: Optical Image of carbon steel: a) without spray b)NaCl c)HCl at the end of week 2

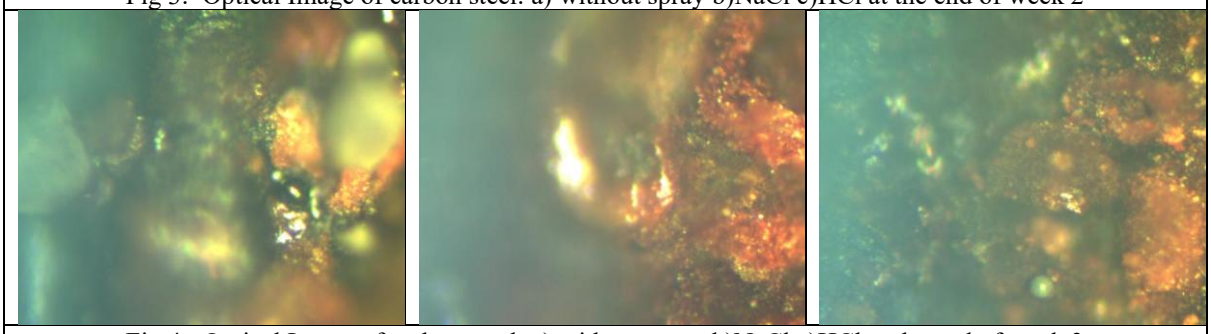

Fig 4: Optical Image of carbon steel: a) without spray b)NaCl c)HCl at the end of week 3

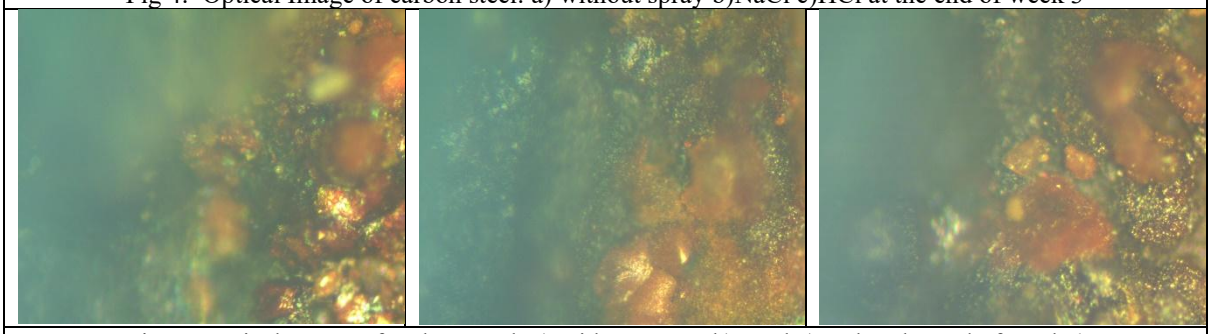

Fig 5: Optical Image of carbon steel: a) without spray b)NaCl c)HCl at the end of week 4

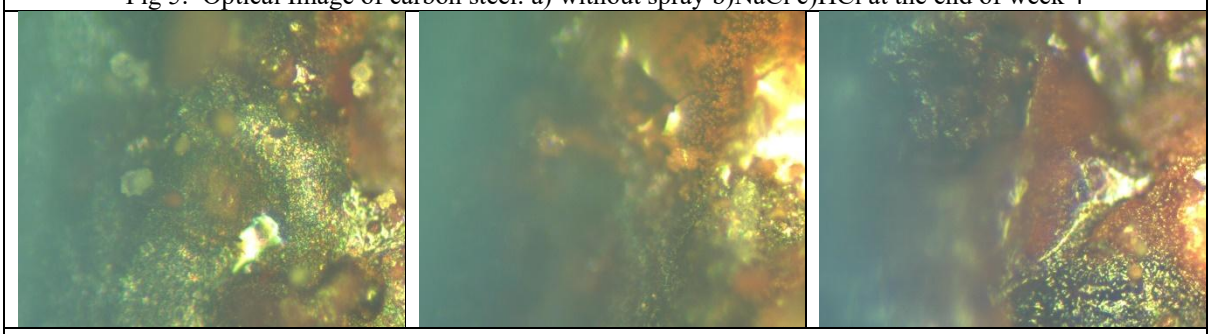

Fig 6: Optical Image of carbon steel: a) without spray b)NaCl c)HCl at the end of week 5

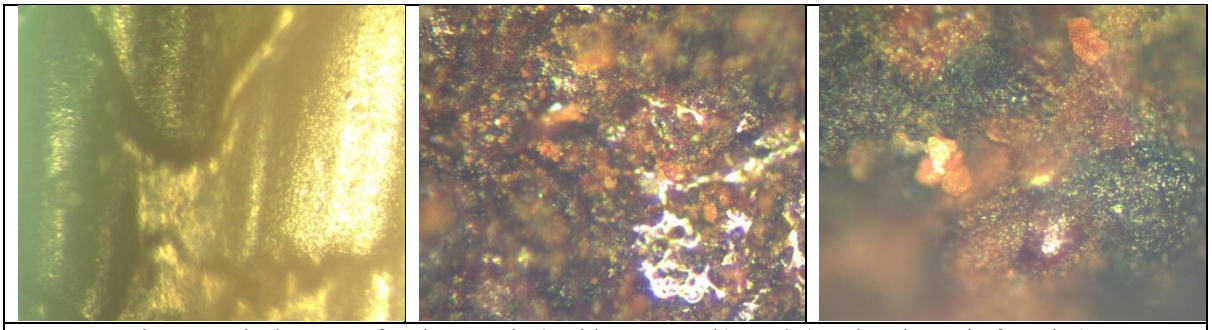

Fig 7: Optical Image of carbon steel: a) without spray b)NaCl c)HCl at the end of week 6

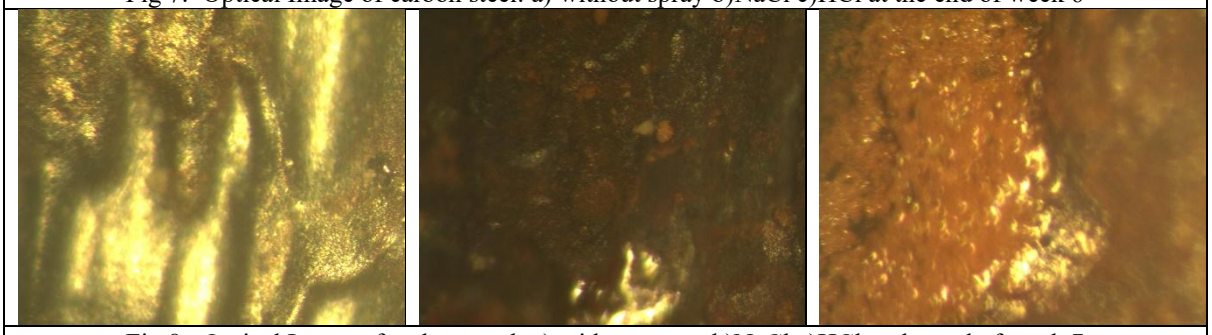

Fig 8: Optical Image of carbon steel: a) without spray b)NaCl c)HCl at the end of week 7

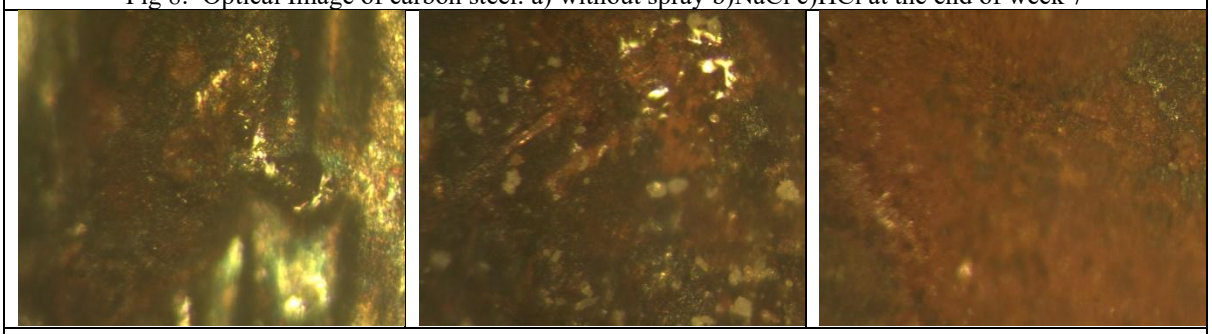

Fig 9: Optical Image of carbon steel: a) without spray b)NaCl c)HCl at the end of week 8

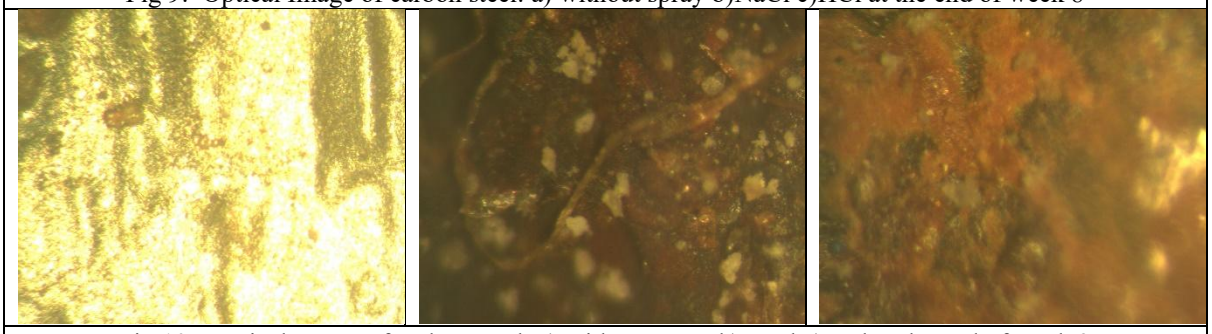

Fig 10: Optical Image of carbon steel: a) without spray b)NaCl c)HCl at the end of week 9

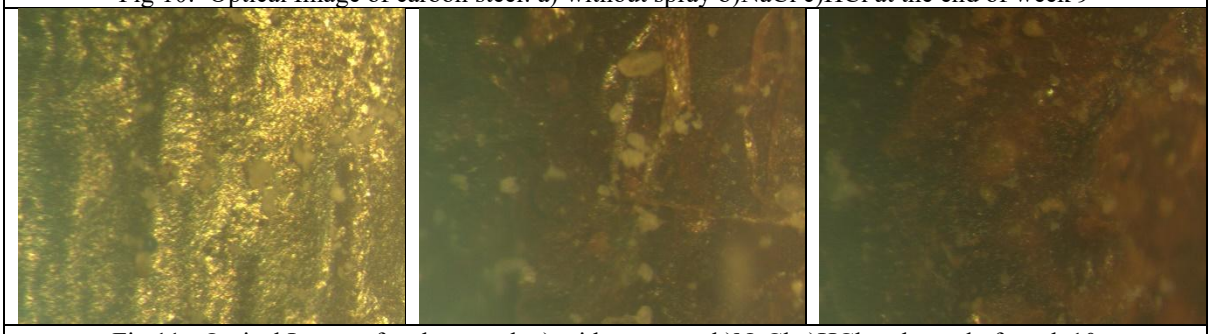

Fig 11: Optical Image of carbon steel: a) without spray b)NaCl c)HCl at the end of week 10

The optical micrographs of carbon steel specimens (Figures 2–11) provide a visual progression of surface degradation under different environmental exposures over a 10-week period. In the control group (without spray), minimal surface changes were observed throughout the study. The surface retained its relative integrity, showing only minor discoloration and a few micro-pits in the later weeks, suggesting natural oxidation under ambient conditions without aggressive corrosion stimuli.

In contrast, the specimens exposed to 4% sodium chloride (NaCl) spray exhibited moderate but progressive corrosion. By Week 2, early signs of surface roughening and pitting were evident, with these effects intensifying in subsequent weeks. The presence of localized rust and increased pit density by Week 5 indicated the onset of chloride-induced localized corrosion, which is typical for NaCl environments due to the aggressive nature of chloride ions in penetrating passive films and promoting pit nucleation. By Week 10, the NaCl-exposed specimens showed widespread corrosion with significant surface roughness and damage, consistent with salt-spray-induced pitting.

The most aggressive corrosion behavior was observed in samples exposed to 36% hydrochloric acid (HCl) spray. As early as Week 1, surface etching and localized attack were apparent. By Week 3, severe surface deterioration and deep corrosion grooves were visible, indicating active material dissolution. The acidic environment not only removed protective oxide layers but also accelerated uniform and localized attack, leading to extensive damage. By Week 10, the HCl-exposed samples displayed heavily corroded surfaces with major material loss and extensive roughening, confirming HCl's highly corrosive impact on carbon steel.

Overall, the optical images clearly demonstrate that corrosion severity increases in the following order: no spray < NaCl spray < HCl spray. These visual findings align with the quantitative corrosion rate and impact strength data, affirming that the corrosion environment significantly influences material integrity over time.

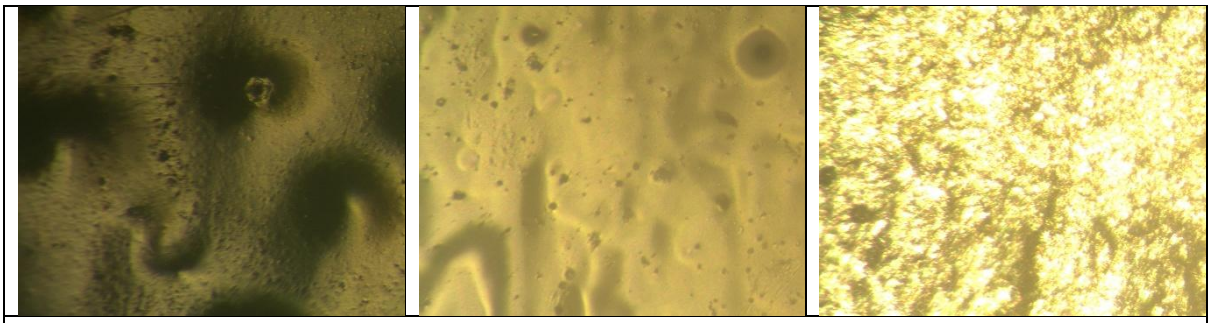

Fig 12: Optical Image of carbon steel coated with: a) paint b) Acrylic c) Zinc at the end of week 1

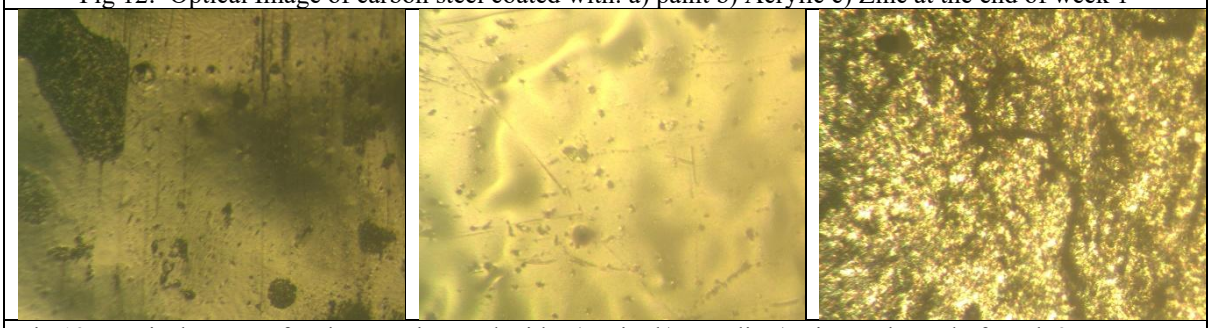

Fig 13: Optical Image of carbon steel coated with: a) paint b) Acrylic c) Zinc at the end of week 2

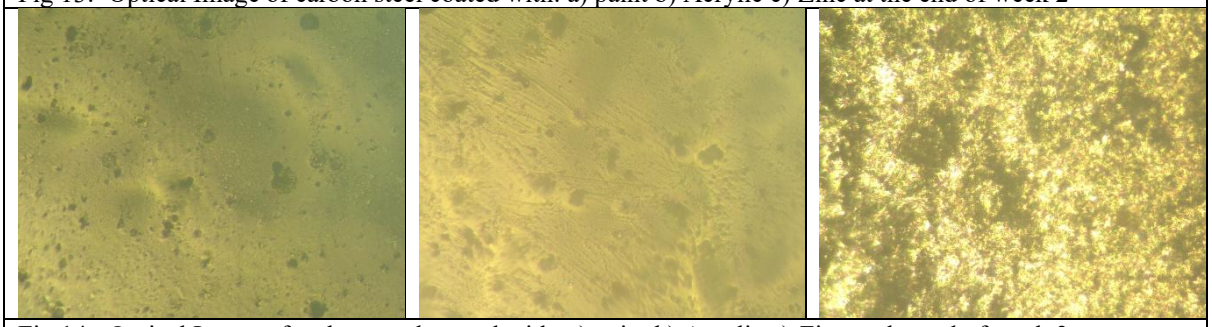

Fig 14: Optical Image of carbon steel coated with: a) paint b) Acrylic c) Zinc at the end of week 3

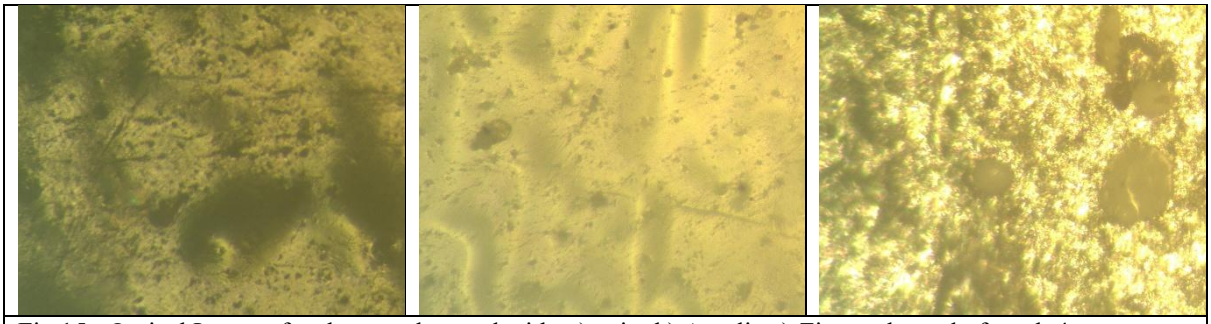

Fig 15: Optical Image of carbon steel coated with: a) paint b) Acrylic c) Zinc at the end of week 4

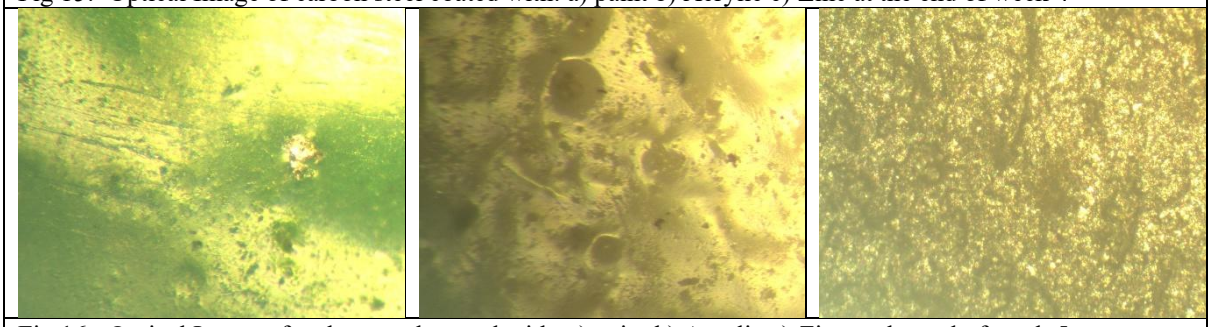

Fig 16: Optical Image of carbon steel coated with: a) paint b) Acrylic c) Zinc at the end of week 5

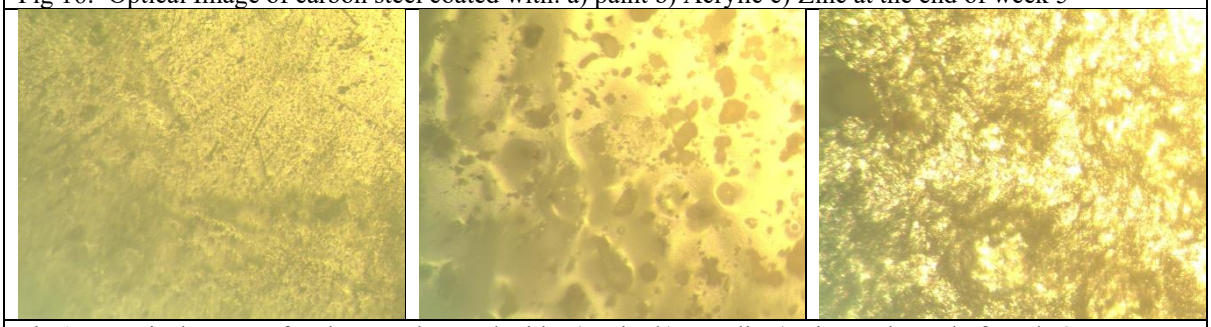

Fig 17: Optical Image of carbon steel coated with: a) paint b) Acrylic c) Zinc at the end of week 6

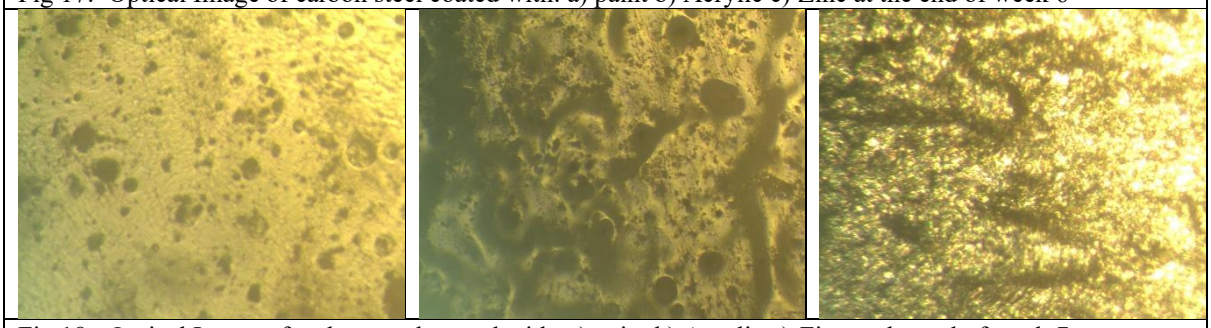

Fig 18: Optical Image of carbon steel coated with: a) paint b) Acrylic c) Zinc at the end of week 7

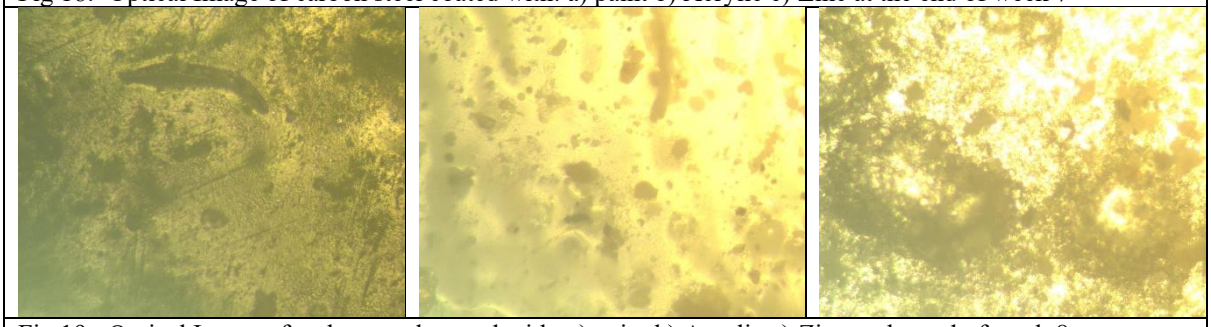

Fig 19: Optical Image of carbon steel coated with: a) paint b) Acrylic c) Zinc at the end of week 8

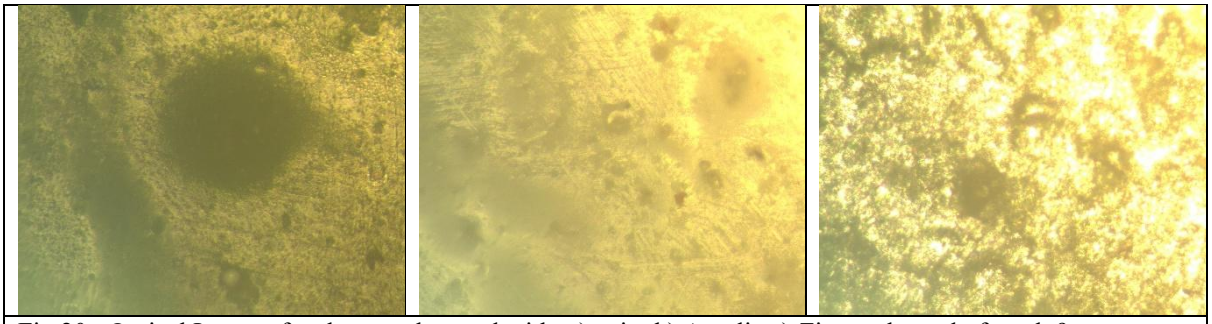

Fig 20: Optical Image of carbon steel coated with: a) paint b) Acrylic c) Zinc at the end of week 9

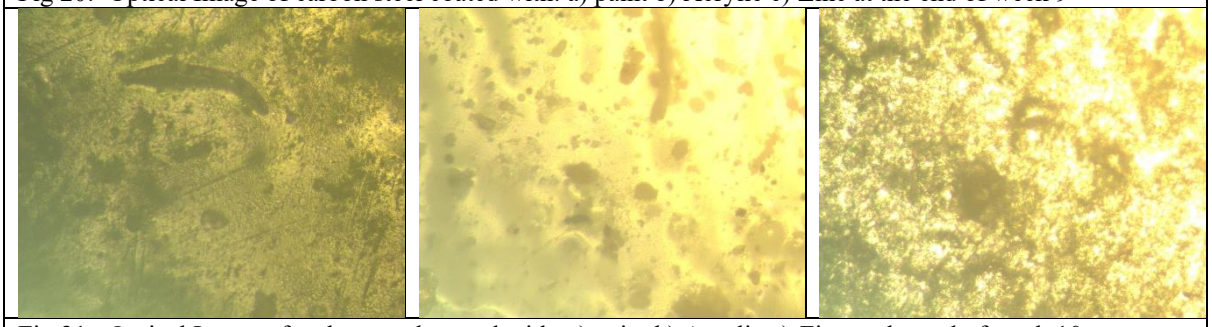

Fig 21: Optical Image of carbon steel coated with: a) paint b) Acrylic c) Zinc at the end of week 10

The optical images (Figures 12–21) depict the surface condition of carbon steel samples coated with paint, acrylic, and zinc, observed weekly over a period of ten weeks. During the initial three weeks, all three coatings maintained relatively stable appearances, with minimal signs of degradation. The paint-coated samples exhibited a uniform and intact surface, while the acrylic coating maintained a glossy finish with no significant changes. Zinc-coated specimens appeared matte grey with no visible corrosion, indicating the coatings were effective in the early stages.

From week four onward, noticeable differences in performance began to emerge. The paint coating started showing minor discoloration and edge blistering, suggesting the onset of moisture penetration. Acrylic coatings, being more susceptible to environmental exposure, began to display haziness and slight underfilm corrosion. Meanwhile, the zinc coating exhibited early signs of white rust—indicative of sacrificial oxidation—but the underlying steel remained unaffected. By week six, degradation in the acrylic samples had progressed considerably, with evident detachment and rust formation beneath the coating layer.

In the later stages, from week seven to week ten, the paint-coated samples demonstrated increased rust formation and weakening of adhesion, particularly around edges and defects. The acrylic-coated specimens deteriorated further, with extensive peeling and widespread corrosion, indicating a significant failure in protective performance. In contrast, zinc coatings continued to protect the base metal effectively; although white rust formation increased, no visible corrosion of the steel substrate was observed.

By week ten, the comparative analysis clearly established that zinc coating offered the most effective long-term protection due to its galvanic sacrificial behavior. The paint coating provided moderate resistance but showed signs of breakdown in extended exposure. Acrylic coating, while initially stable, failed to sustain protective integrity under prolonged environmental conditions. These observations highlight the superior durability of zinc as a protective coating for carbon steel in corrosive environments, followed by paint, with acrylic proving the least effective among the three.

IV. Conclusion

In Salalah's coastal environment, salt-laden air, high humidity, and intense heat create an aggressive corrosion regime for carbon steel. Marine atmospheres like Oman's induce chloride-driven rust phases (for example, akaganeite) that rapidly breach unprotected metal surfaces. In accelerated salt-spray tests, all uncoated samples corroded heavily, but the coated panels showed distinct durability differences. Zinc-rich (galvanized) coatings gave far superior performance: they remained largely corrosion-free even after prolonged exposure, consistent with the observation that "inorganic zinc primers are the primary protective coating for carbon steel at marine/coastal environments". The water-based acrylic system initially impeded rusting, but it began to fail sooner than the zinc system, reflecting its shorter service life. By contrast, the standard organic paint provided minimal defense: its barrier failed quickly under Salalah's conditions, which aligns with the expected lifespan of simple paint coatings and the lack of any sacrificial component. Overall, the rank order of durability observed was zinc >> acrylic > ordinary paint in this severe marine environment.

These findings underscore the critical importance of selecting robust protective systems for infrastructure exposed to Salalah-like conditions. Design specifications should favor zinc-rich primer systems followed by high-performance topcoats (epoxy or polyurethane) rated for severe marine (ISO 12944-C5) environments, with rigorous surface preparation and adequate film thickness. Complementary corrosion-mitigation measures are also recommended: for example, coastal design guidelines note that cathodic protection, when combined with factory-applied coatings, can "effectively prevent corrosion in the submerged zone". Oman's industry experts likewise advocate comprehensive solutions – for instance, pipelines use advanced coatings and corrosion-resistant alloys, desalination plants deploy smart monitoring and anti-fouling materials, and port structures use marine-grade paints – in order to dramatically extend service life and cut maintenance costs. In practice, this means planning routine inspection and re-coating cycles and designing with corrosion allowances or cathodic systems as needed.

References

[1]. Alcántara, J., de la Fuente, D., Chico, B., Simancas, J., Díaz, I., & Morcillo, M. (2017). Marine atmospheric corrosion of carbon steel: A review. *Materials*, 10(4), 406. https://doi.org/10.3390/ma10040406

[2]. López-Ortega, A., Bayón, R., & Arana, J.L. (2019). Evaluation of protective coatings for high-corrosivity category atmospheres in offshore applications. *Materials*, 12(8), 1325. https://doi.org/10.3390/ma12081325

[3]. Popescu, A.M., Demidenko, O., Yanushkevich, K., Donath, C., Neacsu, E.I., & Constantin, V. (2022). Influence of seawater corrosion on structure and magnetic properties of the SR355JR and S355J2 carbon steels. *Journal of the Mexican Chemical Society*, 66(4), 300–311. https://doi.org/10.29356/jmcs.v66i4.1695

[4]. Gao, J., Wang, N., Chen, H., & Xu, X. (2023). The influence of 1 wt.% Cr on the corrosion resistance of low-alloy steel in marine environments. *Metals*, 13(6), 1050. https://doi.org/10.3390/met13061050

[5]. Montemor, M.F. (2014). Functional and smart coatings for corrosion protection: A review of recent advances. *Surface and Coatings Technology*, 258, 17–37. https://doi.org/10.1016/j.surfcoat.2014.06.031

[6]. Refait, P., Grolleau, A.M., Jeannin, M., Rémazeilles, C., & Sabot, R. (2020). Corrosion of carbon steel in marine environments: Role of the corrosion product layer. *Corrosion Materials and Degradation*, 1(1), 198–218. https://doi.org/10.1016/j.cormad.2020.01.001

[7]. Tian, F., He, X., Bai, X., et al. (2020). Electrochemical corrosion behaviors and mechanism of carbon steel in the presence of acid-producing bacterium *Citrobacter farmeri* in artificial seawater. *International Biodeterioration & Biodegradation*, 147, 104872. https://doi.org/10.1016/j.ibiod.2019.104872

[8]. Liu, H., Chen, C., Asif, M., et al. (2022). Mechanistic investigations of corrosion and localized corrosion of X80 steel in seawater comprising sulfate-reducing bacteria under continuous carbon starvation. *Corrosion Communications*, 8, 70–80. https://doi.org/10.1016/j.corcom.2022.08.002

[9]. Sherif, E.S.M., Erasmus, R.M., & Comins, J.D. (2010). In situ Raman spectroscopy and electrochemical techniques for studying corrosion and corrosion inhibition of iron in sodium chloride solutions. *Electrochimica Acta*, 55(10), 3657–3663. https://doi.org/10.1016/j.electacta.2010.01.117

[10]. Oh, S.J., Cook, D.C., & Townsend, H.E. (1998). Characterization of iron oxides commonly formed as corrosion products on steel. *Hyperfine Interactions*, 112(1), 59–66. https://doi.org/10.1023/A:1011076308501

[11]. Sherif, E.S.M. (2014). A comparative study on the electrochemical corrosion behavior of iron and X-65 steel in 4.0 wt% sodium chloride solution after different exposure intervals. *Molecules*, 19(7), 9962–9974. https://doi.org/10.3390/molecules19079962

[12]. Tejero-Martín, D., Rezvani Rad, M., McDonald, A., & Hussain, T. (2018). Beyond traditional coatings, a review on thermal sprayed functional and smart coatings. arXiv:1811.05289

[13]. Yu, F., Camilli, L., Wang, T., et al. (2018). Complete long-term corrosion protection with chemical vapor deposited graphene. arXiv:1805.05102

[14]. Saidi, R., et al. (2020). Research progress of marine anti-corrosion and wear-resistant coating. *Progress in Organic Coatings*. https://doi.org/10.1016/j.porgcoat.2020.105641

[15]. Collazo, A., Díaz, B., Figueroa, R., Nóvoa, X.R., & Pérez, C. (2024). Corrosion resistance of a water-borne resin doped with graphene derivatives applied on galvanized steel. arXiv:2401.15410